DEUTSCHES ELEKTRONEN – SYNCHROTRON

DESY 92-121
August 1992

Introduction to Radiation Backgrounds in a B Factory

S. Khan

Max-Planck-Institut für Kernphysik, Heidelberg

ISSN 0418-9833

NOTKESTRASSE 85 · D-2000 HAMBURG 52

To be sure that your preprints are promptly included in the
HIGH ENERGY PHYSICS INDEX,
send them to (if possible by air mail):

DESY **Bibliothek** **Notkestraße 85** **W-2000 Hamburg 52** **Germany**	**DESY-IfH** **Bibliothek** **Platanenallee 6** **O-1615 Zeuthen** **Germany**

DESY 92-121
August 1992

ISSN 0418-9833

Introduction to Radiation Backgrounds in a B Factory*

Shaukat Khan
Max-Planck-Institut für Kernphysik, W-6900 Heidelberg 1, FRG

ABSTRACT

Detector backgrounds in a B Factory due to synchrotron radiation and beam-gas interactions are discussed and the computational tools to simulate these processes are outlined. As an example of their application, simulations and beam tests that preceded the installation of the ARGUS silicon vertex detector are described.

1. INTRODUCTION

The requirement of acceptable background conditions in a B factory detector is one of the main issues in the layout of the machine and the design of the central part of the detector. There are two major sources of radiation backgrounds:

1) Synchrotron radiation (SR) is emitted wherever the beam is bent or focussed. The high luminosity required to reach the physics goals of a B factory implies high beam currents and a small beam spot at the interaction point (IP). Since the intensity of a single bunch is limited, high currents are achieved by using a large number of bunches. A fast beam separation to prevent parasitic bunch crossings as well as focussing to achieve a small beam spot make the generation of SR in the vicinity of the detector unavoidable.

2) Interactions with the residual gas cause beam particles to leave their orbit due to deflections (Coulomb scattering) and radiative energy losses (bremsstrahlung). These 'lost' particles as well as bremsstrahlung photons emitted near the IP initiate electromagnetic showers when hitting the beam pipe and may send shower debris into the detector.

The high rate of Bhabha events as another potential source of considerable radiation is discussed in [1].

The radiation problem could be avoided if the beam pipe within the detector could be arbitrarily large. However, good vertex resolution as another vital requirement of a B factory demands a small beam pipe radius. Furthermore, a thin beam pipe to minimize multiple Coulomb scattering is highly transparent to SR photons. The layout of the interaction region is a compromise between the conflicting requirements of high luminosity, moderate background and good vertex resolution.

For a given machine lattice and masking geometry, the amount of radiation emitted and absorbed during luminosity running conditions can be estimated by Monte-Carlo simulations. The radiation level during machine studies, injection or commissioning is beyond the scope of any simulation. Here, one can only extrapolate from the experience gained with existing machines.

Monte-Carlo studies for the proposed B factories are described in other contributions to this conference and their discussion shall be omitted here. Instead, the work that preceded the installation of the ARGUS silicon vertex detector may serve as an instructive example. The lattice and detector geometry is less complex than in a B factory and the results of Monte-Carlo programs applied to an existing machine can be verified by measurements. For a B factory, the reliability of the background prediction is a question of vital importance.

2. LIMITS ON RADIATION BACKGROUNDS

Showers from lost beam particles and SR photons may damage the detector and add to the occupancy, the probability of background hits overlapping with real tracks. Background limits are given by the radiation hardness of a sensitive detector component, the period of time it should survive and the max-

*Talk at SLAC Conference on B Factories: State of the Art in Accelerators, Detectors and Physics, April 6-10, 1992.

imum acceptable occupancy. Furthermore, the absorbed SR power adds to the heat load and must be limited to values, for which cooling can be provided. A further limit to consider for lost beam particles is the number of background events that pass the first level trigger and may cause dead time.

The radiation dose and occupancy limits may be expressed in different ways, as illustrated by the following example (see also [2]):

Silicon strip detectors are read out by radiation sensitive VLSI chips. Contemporary chips survive 200-500 Gy (=J/kg). For one year of operation, the dose limit may be expressed as 0.1 Gy/h or $2.8 \cdot 10^{-8}$ W/g. On a 200 μm thick layer of silicon, this corresponds to $1.3 \cdot 10^{-9}$ W/cm^2 being absorbed. Consider the simple case, where SR is the major background source and the spectrum is dominated by 8 keV photons, e.g. from fluorescence in a copper layer on the beam pipe. In this case, the limits given above correspond to 10^6 absorbed photons/(cm^{2}s). The occupancy related to a given number of hits per time and area depends on the detector segmentation and integration time. For a 10 cm long and 0.03 cm wide area on a strip detector being affected by a background hit and an integration time of 100 ns, the present case leads to 3% occupancy.

In this example, more radiation hard chips (which do already exist) would not allow to push the limits higher, because the occupancy is already large. In the case of a pixel detector, however, the area affected by a background hit is much smaller and a higher hit density could be tolerated.

In practice, the usefulness of such an estimate is rather limited, since the spatial and energy distribution of radiation will usually be quite complex and has to be determined by a detailed Monte-Carlo simulation.

3. The Simulation of Radiation

3.1 Monte-Carlo Programs

The simulation of either type of radiation requires a ray tracing program that follows individual particle trajectories through the machine lattice. In the case of SR, it may be sufficient to consider the last 10 m upstream of the IP and several ray tracing programs that generate SR are in use (e.g. SYNCBKG [3]). In the case of scattered beam particles, a more thorough treatment of the machine lattice is required, since charged particles can travel several hundreds of meters down the beam line before hitting the wall. A popular program that tracks the initial beam particles as well as particles having suffered an interaction with the residual gas is DECAY TURTLE [4].

Simulating the interaction of the emitted radiation with matter can be difficult and time-consuming, depending on how accurate the various interactions are treated and in how much detail the true detector geometry is modelled. Most of the ray tracing programs are restricted to the more machine-related job of radiation production. Their output has to be interfaced to a program that treats the detector-related part of radiation absorption. EGS4 [5] is a code that is widely used for this purpose.

In the case of SR, a few programs simulate the emission as well as the absorption of photons in the detector [6].

3.2 Ray Tracing

At a given location along the beam line, a Gaussian transverse particle distribution is conveniently defined by two elliptical boundaries in the horizontal and vertical phase space coordinates (x, x') and (y, y'), respectively. At the IP, the beam envelope usually has a waist and the phase space ellipses are upright (as in fig.1a). In this case, the 1-σ extent of the beam in real and momentum space is given by the emittances ϵ_x and ϵ_y and the values of the beta-functions β_x^* and β_y^* at the IP:

$$\sigma_x = \sqrt{\epsilon_x \cdot \beta_x^*} \qquad \sigma_{x'} = \sqrt{\epsilon_x / \beta_x^*}$$

and likewise for y and y'. Once these parameters are known, a ray-tracing program can start from the IP at randomly chosen points (x, x', y, y') within a, say, 10-σ envelope. The choice of the method of sampling these points is important, because the particle density varies by many orders of magnitude. Chosing the transverse coordinates with a Gaussian random number generator enhances the central region of the beam, but may neglect potentially important regions several σ from the beam axis, whereas a flat sampling distribution may lead to spending most of the computation time on insignificant contributions.

The horizontal and vertical coordinates are to first order independent from each other. The coordi-

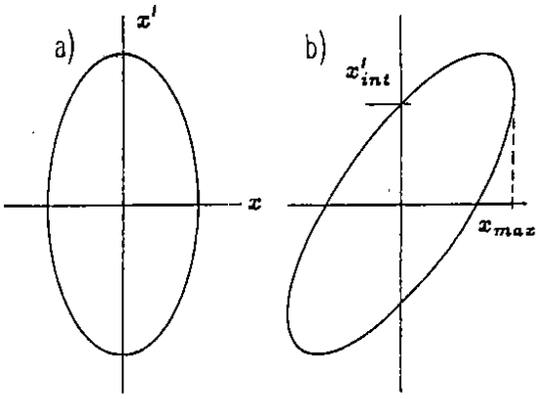

Figure 1: Emittance ellipses: a) at the IP, where the beam has a waist, and b) a general case, where $\sigma_{x'} = x'_{int} = (\epsilon_x/\beta_x)^{1/2}$.

nates (x, x') and (y, y') at one longitudinal location are easily transformed into coordinates at another location by the successive application of two-dimensional transfer matrices. For example, tracing through a drift space of length L, followed by a horizontally defocussing (vertically focussing) quad of length l and strength k^2 requires the transformations (see e.g. [7])

$$\begin{pmatrix} x \\ x' \end{pmatrix} = \begin{pmatrix} \cosh kl & \frac{1}{k}\sinh kl \\ k\sinh kl & \cosh kl \end{pmatrix} \begin{pmatrix} 1 & L \\ 0 & 1 \end{pmatrix} \begin{pmatrix} x \\ x' \end{pmatrix}_{\rm IP}$$

$$\begin{pmatrix} y \\ y' \end{pmatrix} = \begin{pmatrix} \cos kl & \frac{1}{k}\sin kl \\ -k\sin kl & \cos kl \end{pmatrix} \begin{pmatrix} 1 & L \\ 0 & 1 \end{pmatrix} \begin{pmatrix} y \\ y' \end{pmatrix}_{\rm IP}$$

This is illustrated by fig.2, showing a horizontal and vertical view of random trajectories through the ARGUS IP and the mini-β-quad (L = 1.26 m, l = 0.88 m, $k^2 = 1.12\ \mathrm{m}^{-2}$).

Dipole magnets introduce a slight complication, since here the orbit is curved and the 'beam system' with one axis tangential to the orbit does no longer coincide with the lab system. An additional transformation is required for off-axis quadrupoles, since the above given matrices are valid only in a system centered at the magnet's axis. Off-axis quads are used in various B factory designs to perform the combined function of focussing *and* beam separation.

3.3 Emission of Synchrotron Radiation

SR photons are emitted nearly tangential to the beam particle trajectory. The average angular deviation of $1/\gamma$ is negligible for B factory energies. The mean number N_γ of photons emitted per meter is

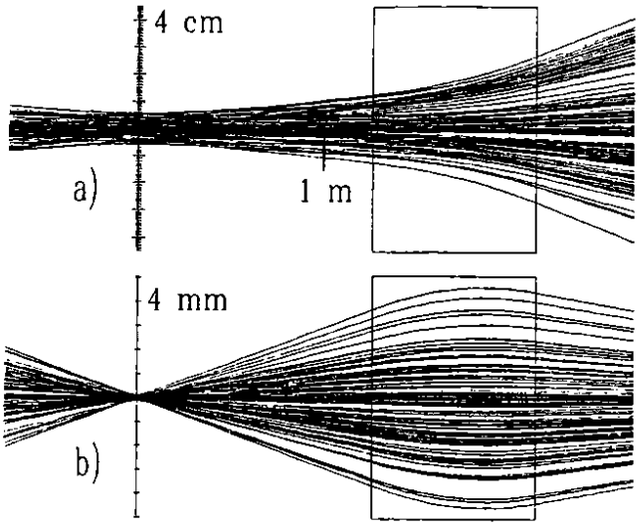

Figure 2: Horizontal (a) and vertical (b) view of random electron trajectories through the IP and the *mini-β*-quadrupole of ARGUS.

$$N_\gamma = 20.6\ E_{beam}/r$$

where the bending radius r is measured in m and the beam energy in GeV. The mean photon energy $\langle E_\gamma \rangle$ in keV is given by

$$\langle E_\gamma \rangle = 0.308\ E_c \quad \text{with} \quad E_c = 2.218\ E^3_{beam}/r.$$

E_c is called the critical energy. Combining N_γ with the mean energy yields the well-known result of the SR power being $\sim E^4_{beam}/r^2$.

The spectrum of SR power and the photon number distribution is shown in fig.3 (for analytical expressions see e.g. [7] or [8]). The accuracy requirements for sampling photons from the spectrum are moderate, since the result will usually be dominated by the statistical error: contributions of a few nW are important for sensitive detector components, whereas the SR power generated in the interaction region of a B factory is expressed in kW.

The amount of SR generated in quadrupole magnets is increased, if the beam profile has non-Gaussian tails. The exact shape of a beam is hard to predict, but to simulate a flat beam tail the parametrization

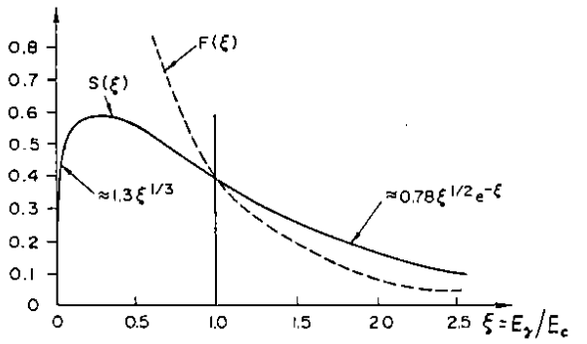

Figure 3: SR photon number $F(\xi)$ and power $S(\xi)$ versus photon energy ξ in units of the critical energy E_c (from [7]).

$$dN/dx = e^{-x^2/2\sigma_x^2} + Ae^{-x^2/2(10\sigma_x)^2}$$

may be used for the transverse electron number distribution in x and likewise in y [3]. For the ARGUS *mini-β*-quad, the radial distribution of SR that would reach the IP if no apertures were present is shown in fig.4 for different values of A. In the case of a purely Gaussian beam profile, the distribution is very narrow, as can be guessed from the trajectories in shown in fig.2. Most of the SR encountered at a relevant radius ~10 mm is due to the third upstream quad. At this radius, the SR from the first quad rises by an order of magnitude for $A = 10^{-3}$ (which may be unrealistically large), whereas the amount of SR received from all magnets increases by just a factor of two. The situation may be different for other lattice geometries.

3.4 Beam-gas Interactions

Coulomb scattering off the nuclei of the residual gas causes an angular deflection of beam particles by an angle Θ. The emission of bremsstrahlung in the vicinity of a nucleus leads to an energy loss ϵ. Approximate expressions for the differential cross sections are

$$\frac{d\sigma}{d\Omega} = 4\, r_e^2\, Z^2\, \gamma^{-2}\, \Theta^{-4}$$

for Coulomb scattering into small angles and neglecting screening effects and

$$\frac{d\sigma}{d\epsilon} = \frac{4}{137}\; r_e^2\, Z^2\, \frac{1}{\epsilon}\; F(E_{beam}, \epsilon, Z)$$

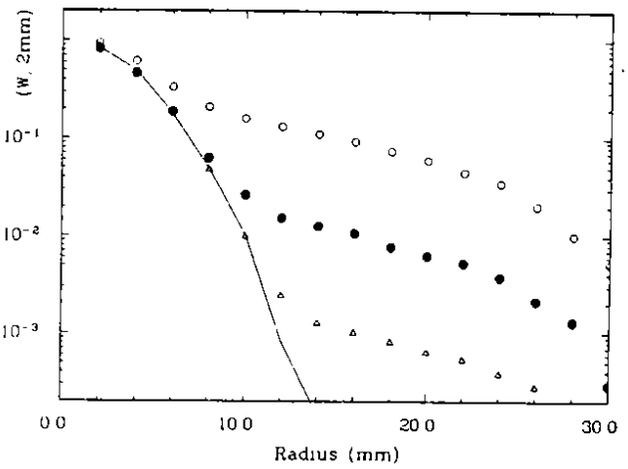

Figure 4: Radial distribution of SR from the ARGUS *mini-β* quadrupole for different contributions of a flat beam tail, described by the parameters A. — $A = 0$; < $A = 10^{-5}$; • $A = 10^{-4}$; ○ $A = 10^{-3}$.

for bremsstrahlung, where r_e is the classical electron radius, Z the atomic number and F is a slowly varying function, which approaches $4/3\ \ln(183/Z^{1/3})$ for $\epsilon \approx 0$ (see e.g. [8] for a detailed discussion). Since these cross sections fall off rapidly with Θ and ϵ, the probability of an event with significant energy loss *and* considerable scattering angle is the product of two small numbers. A separate treatment of these processes is therefore justified. When using the program DECAY TURTLE, a parameter invokes either bremsstrahlung or Coulomb scattering.

3.5 The Absorption of Radiation

Once a SR photon, a lost beam particle or a bremsstrahlung photon enters the material of the beam pipe and the detector, it will loose energy in a number of scattering processes. Cross section and angular characteristics of these processes depend on the energy of the incident particle and on the atomic number of the material traversed.

Photons undergo Rayleigh and Compton scattering, photoelectic absorption and pair production. For SR at B factory energies, pair production can be neglected. In the relevant energy region for SR photons of 1-100 keV, atomic binding effects should not be ignored in Rayleigh and Compton scattering. The differential cross sections

$$\frac{d\sigma_{Rayleigh}}{d\Omega} = \frac{d\sigma_{Thomson}}{d\Omega} \; |F(q,Z)|^2$$

and

$$\frac{d\sigma_{Compton}}{d\Omega} = \frac{d\sigma_{K.N.}}{d\Omega} \; S(q,Z)$$

are modified with respect to the free-electron cross sections (Thomson and Klein-Nishina) by scattering functions $S(q,Z)$ and form factors $F(q,Z)$, respectively, where q is the recoil momentum [9].

Electrons and positrons are subject to energy losses due to inelastic atomic collisions and bremsstrahlung and to angular deflections from multiple Coulomb scattering. Electromagnetic showers can be viewed as a chain of alternate pair production and bremsstrahlung processes.

Furthermore, the magnetic field of the detector has to be included. Charged particles of low energy curl up and may hit the same structure several times.

The determination of the radiation dose experienced by a given detector component requires a detailed simulation of all these processes in a realistic model of the detector geometry. The radiation dose, i.e. the absorbed energy divided by the mass of an object, is not a property of a given environment. It depends on the atomic number, but also on the size and shape of an object, since the absorbed energy is generally not proportional to the mass.

4. Measures against Radiation Backgrounds

The task of reducing the radiation background may be divided into two parts:

1) The more machine-related part is to minimize the generation of radiation that may enter the detector.

SR, if not avoidable, should be directed away from the detector or should pass it in a small cone without too many photons hitting the walls. In the layout of the interaction region, a tilted detector solenoid field and quadrupoles with the incoming (outgoing) beam on-axis (off-axis) may be employed for this purpose.

Radiation from beam-gas interactions is reduced by improving the vacuum and introducing scrapers at suitable positions, e.g. where the dispersion and therefore the transverse displacement of off-momentum particles is large.

2) On the detector side, the background from either source can always be reduced by increasing the beam pipe diameter.

In the case of SR, direct radiation is easily attenuated by masks, whereas the difficulty lies in optimizing the mask positions, shapes and materials to minimize the number of photons leaking through the mask tips or being backscattered into the detector.

In order to reduce the radiation received from electromagnetic showers, two complementary strategies may be followed. One strategy is to minimize, the other is to maximize the amount of the material in which the shower develops. In either case, the material thickness in front of a sensitive detector component should not be close to 5-10 radiation lengths, where the shower maximum i.e. the highest energy deposition per length occurs.

5. Radiation Shielding of the ARGUS Si Vertex Detector

5.1 History

In spring 1990 the ARGUS detector was upgraded by installing a new micro vertex drift chamber (μVDC) together with a (Ø38 × 0.5) mm Be beam pipe. At the same time, a silicon detector within the μVDC had been proposed, which required an even smaller beam pipe. Therefore, a (Ø15 × 0.15) mm Al pipe was tested at the DORIS storage ring in May 1990. It was demonstrated that the operation of DORIS with such a small aperture was feasible, but the radiation of 70-100 Gy/h in the vicinity of the Al pipe was by far exceeding values at which a Si detector could be operated. It was decided to pursue the project nevertheless, but due to a major shutdown of DORIS the development of a beam pipe with reduced background relied exclusively on a Monte-Carlo simulation. One objective of the simulation was to understand the high amount of radiation experienced during the test, the other aim was to reduce the radiation level by three orders of magnitude. The results were verified one year later in a beam test and the silicon detector was successfully operated during a short run in October 1991. For the coming ARGUS run period, the design of the silicon detector was modified and a new device was installed in May 1992.

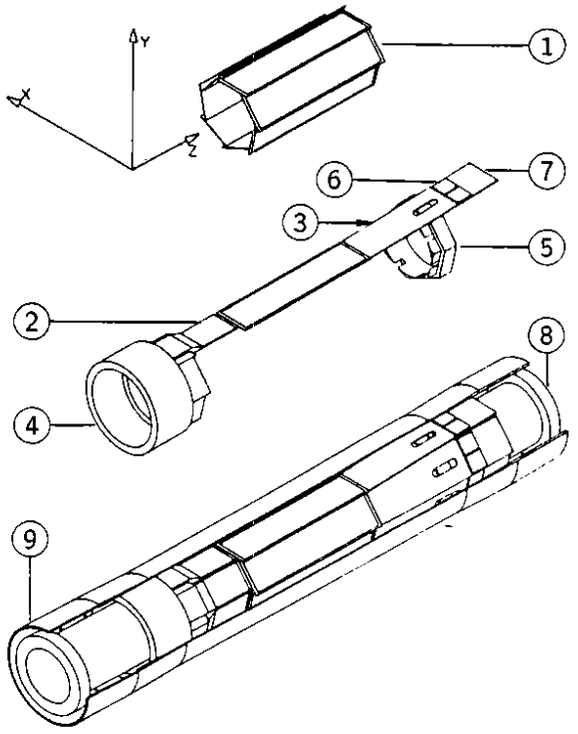

Figure 5: The ARGUS silicon vertex detector.
1) Si detectors. 2) Support bar. 3) Support bar with adapter between detector and chips. 4,5) Support rings. 6,7) Readout chips and hybrid. 8) Beam pipe with Al-steel connection at both ends. 9) Carbon fibre tube of the μVDC.

5.2 Detector Layout

The ARGUS silicon vertex detector consists of seven individual detector modules, cylindrically arranged around the beam pipe as shown in fig.5. The closest distance between a detector plane and the IP is 12.5 mm. The single-sided strip detectors [10] are 280 μm thick and have an active area of (60.4 $\times$ 12.8) mm^2 each. The 512 strip diodes (25 μm pitch) per detector running parallel to the beam axis are individually biased by polysilicon lines and are AC coupled to the Al readout lines. Every second strip is read out using two VLSI preamplifier chips per detector (in 1991, the MX-3 CMOS chip [11] was employed). A peculiarity of this design is the 40 mm long adapter that connects the chips to the detector. The adapter allows to place the radiation sensitive electronics at a position of reduced radiation and to put shielding material between the chips and the beam pipe. In 1991, this gap was occupied by a tungsten shield of $\sim$25 radiation lengths along the beam axis to attenuate electromagnetic showers. The opposite strategy will be followed in the next running period using a low-material beam pipe.

The silicon vertex detector occupies the space between a (Ø38 $\times$ 0.5) mm carbon fibre tube that replaces the former Be beam pipe, and the new Al (Ø22 $\times$ 0.20) mm beam pipe. SR masks of 18 mm diameter represent the smallest apertures.

5.3 A Monte-Carlo Background Study

Seen from the ARGUS IP, four quadrupole magnets are followed by a very weak dipole magnet. The SR simulation identifies the first (*mini-β*) and the third quad as the major source of radiation. Fig.6 shows two different geometries for which SR was simulated: a) the test beam pipe used in 1990 and b) the new ARGUS beam pipe.

For the test beam pipe the SR simulation yields 50 Gy/h in total (e^+ plus e^-) deposited in a 0.3 mm thick silicon layer wrapped around the thin part of the beam pipe. To account for the slightly larger doses experienced during the test (70-100 Gy/h), only small deviations of the beam from its nominal axis are required. In the simulation of the new beam pipe, a silicon layer around the pipe receives 0.02 Gy/h while the dose at the position of the chips is negligible. This improvement is achieved by increasing the beam pipe diameter from 15 mm to 22 mm and by introducing two sets of SR masks. The outer steel masks at z=$\pm$180 mm are water-cooled and receive the major part of the radiation. The position of the inner titanium masks (z=$\pm$100 mm) is a compromise between shielding from direct radiation and avoiding photons being backscattered from the masks into the detector. Titanium was chosen because the energy of its K-line photons is sufficiently low for fluorescence photons to be attenuated by the 200 μm thick Al tube.

Fig.7 shows the resulting spectra of the radiation power absorbed in the thin part of the respective Al tube and in a surrounding silicon layer. The spectra for the case of the new beam pipe demonstrate that the Ti K-line photons radiated from the SR masks are completely absorbed in the Al tube.

The simulation was repeated for beams off the nominal axis. Large deviations could increase the background at the detector position by one order of magnitude, but would still not endanger the electronics.

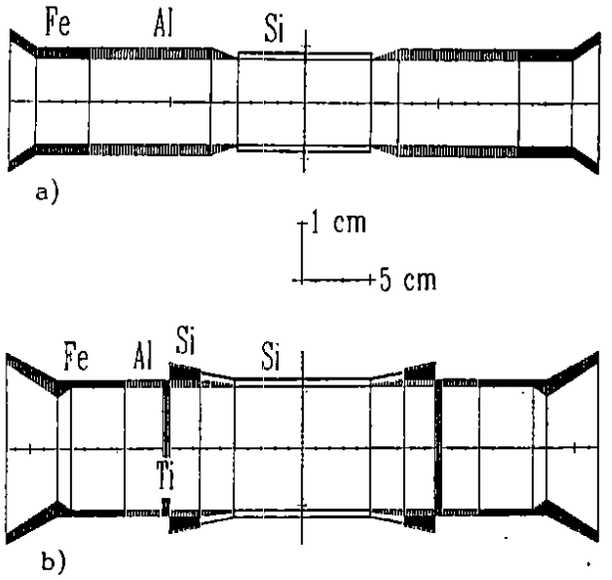

Figure 6: Geometry implemented in the SR simulation program. a) Test beam pipe Al (Ø15 × 0.15) mm and a silicon layer wrapped around it. b) New ARGUS beam pipe Al (Ø22 × 0.2) mm, including a silicon layer, two silicon cones to model the readout chips and part of the tungsten shield against lost beam particles.

The whole storage ring was implemented in a DECAY TURTLE simulation of Coulomb scattering and bremsstrahlung, where the latter process turned out to be dominant. The EGS4 simulation of the showers initiated by lost beam particles included the beam pipe, the silicon detector and different versions of a tungsten shield. In contrast to SR, the energy deposition due to showers does not scale with the particle energy, but with the flux of incident particles, since most of them are minimum-ionizing.

The simulation results in ~20 particles lost per μs. which is compatible with the observed beam life time. On average, one of these particles hits the wall in the interaction region, sometimes after travelling as far as twice around the ring. A radiation level of 0.5 Gy/h determined for the 15 mm beam pipe confirms that SR was the predominant source of radiation experienced in the 1990 test. However, with SR being reduced by a large factor for the new design, the background from beam-gas interactions becomes the larger problem. The simulation predicts 0.18 Gy/h in the Si detector region and 0.05 Gy/h at the chip position, which is just at the limit for 100-200 days of operation.

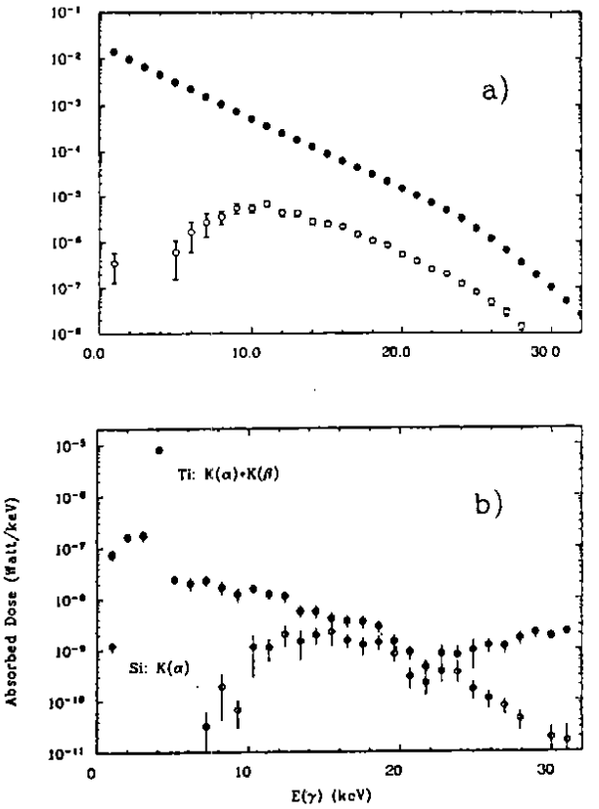

Figure 7: Spectra obtained from the Monte-Carlo simulation for SR power absorbed in the Al beam pipe (black dots) and in the silicon layer (white dots). a) Test beam pipe. b) New ARGUS beam pipe.

5.4 A Beam Test at the ARGUS IP

The Monte-Carlo predictions for beam-gas interactions leave no safety margin. If the background were to exceed the predictions by one order of magnitude, the operation of a silicon detector would be impossible. Therefore, the decision whether to install the new component or not was subject to a test measurement at the ARGUS IP in July 1991.

5.4.1 *Experimental Method*

Energy spectra in time slices of 1-5 minutes were obtained from 12 *pin*-diodes (Siemens BPW 34) mounted in BNC-connectors on three rings around the beam pipe (fig.8). During the test, the position of the two outer rings and the radial position of the diodes was varied. A copper absorber of 1 mm thickness was put in front of the diodes during some runs to distinguish between energy deposition from low and high energy particles. Measurements were performed with and without a tungsten shield (also

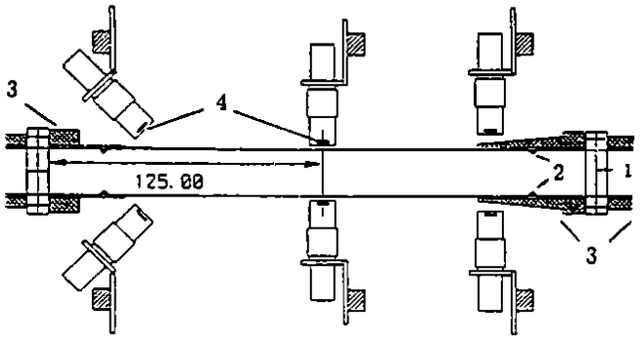

Figure 8: Experimental set-up to measure the radiation background at the ARGUS IP. 1) Al-steel connection. 2) Titanium SR masks. 3) Tungsten shield. 4) Si *pin*-diodes in BNC connectors.

shown in fig.8) surrounding the beam pipe.

Simultaneously, the integral doses were measured at several positions using thermo- and photoluminescence dosimeters. Two gas chambers were installed to monitor the overall radiation level. As second part of the beam test, a silicon detector module identical to the ones made for ARGUS was mounted on the beam pipe and two plastic scintillators served as trigger for charged particles. Finally, the temperature in the vicinity of the silicon detector was measured simulating the enclosement within the μVDC with a plastic tube.

After obtaining the noise spectrum of the *pin*-diodes without beam, the background measurement was started and two electron bunches with a total current of 40 mA were injected. Once the current dropped below 20 mA, the measurement was stopped.

The energy resolution of the diodes as obtained from measuring ^{241}Am photon lines was $\sim$2 keV. The dose measurements in terms of Gy/h per mA of beam current were reproducable on the level of 10%. Time-integrated doses were consistent within a factor of two with the readings of dosimeters put next to the diodes for several hours.

5.4.2 *Results*

The main objective of the beam test was to show that the radiation level permitted the silicon detector to be installed in ARGUS. Radiation doses compatible with the predictions were the immediate results of the *pin*-diode and dosimeter measurements. A strip detector that was placed close to the beam pipe showed no signs of degradation after two days of operation and the cooling provided for the SR masks proved to be adequate. Since no positron beam was available during the test, effects due to the interaction between colliding bunches could not be studied. However, the successful operation of the Si vertex detector in ARGUS confirmed the test results qualitatively.

A detailed comparison of the data with Monte-Carlo simulations in view of their relevance to B factory studies is the subject of a PhD thesis. This is not a straightforward task, since the beam was unstable during the test and the knowledge of the machine parameters as function of time was limited. To gain more information during the coming ARGUS run period, *pin*-diodes have been installed close to the silicon detector. In the following, some preliminary results of the beam test shall be outlined:

Fig.9 shows a typical spectrum obtained from a *pin*-diode. The spectrum of electronic noise measured before injecting the beam has been subtracted. The peak at lower energies is interpreted as SR. As expected for photons of this energy, the peak disappears if the copper absorber is present. Furthermore, its position and width is compatible with the photon energy distribution obtained from the simulation and folded with the diode resolution (also shown in fig.9). The number of hits integrated over the presumed SR peak is generally within a factor of two in agreement with the prediction. Its variation with time and the observed azimuthal asymmetry about the beam axis indicate that the beam position was unstable and slightly off the nominal axis.

The SR peak contributes only little to the energy-weighted spectrum, the integral of which yields the total absorbed energy and corresponds to the radiation dose. As predicted, most of the dose must be attributed to lost beam particles. For stable beam conditions, the radiation level was proportional to the beam current and this correlation persisted during the injection phase. A decrease in beam life time was usually accompanied by an increase in radiation. However, at some instances changes of the radiation level without changes in the beam life time were observed.

Assuming that the energy deposition scales with beam current and life time, the average dose measured above the tungsten shield and normalized to 30 mA and τ=3 h amounted to 0.026 Gy/h. Without the shielding material, 0.079 Gy/h were re-

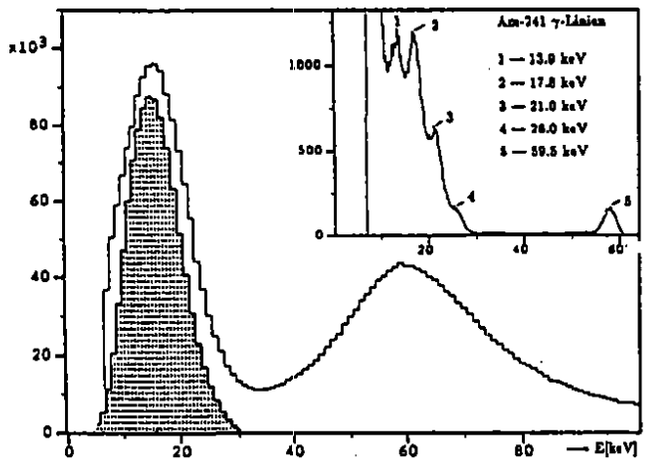

Figure 9: Typical spectrum obtained with Si *pin*-diodes. The peak around 20 keV is compatible with the Monte-Carlo prediction for SR, folded with the diode resolution (hatched area). The resolution of ~2 keV is deduced from the measurement of the ^{241}Am photon spectrum (inset).

ceived. For the same diode position, the EGS4 simulation yields 0.028 (0.054) Gy/h with (without) tungsten shield. Given the complexity of the problem and the uncertainties in the beam parameters, the agreement is remarkably good.

6. CONCLUSIONS

Powerful computational tools exist to simulate the processes that account for the radiation background in e^+e^- collider experiments. The major sources are synchrotron radiation generated in the vicinity of the detector and beam-gas interactions at distinct places, which can be far away from the IP. The latter is the more difficult process to simulate and to fight against: it involves a large part of the machine lattice and the interaction processes in the detector material are more complex than in the case of SR photons. Furthermore, measures against the background from beam-gas interactions yield only small factors, while the reduction of SR due to masking is typically expressed in orders of magnitude. On the other hand, this means that the SR simulation is more sensitive to the accuracy of its input parameters i.e. the size, shape and position of the beam.

The result of a background simulation is generally considered to be accurate within one order of magnitude, which is sufficient for B factory studies, if reasonable safety margins are taken into account.

In the case of the ARGUS study, where the fate of a new detector component depended on the reliability of the simulation, the measurements agreed within a factor of two with the prediction. However, more experimental information on radiation backgrounds and their comparison with Monte-Carlo predictions is desirable. The rising interest in vertex detection at existing or future experiments, where radiation sensitive components have to be placed as close as possible to the beam, will certainly stimulate further experimental studies dedicated to this question in the near future.

REFERENCES:

[1] H. DeStaebler, this conference.
[2] Th. Browder and M. Witherell, CLNS 90-1019 (1990).
[3] An Asymmetric B Factory Based on PEP, SLAC-372 (1991).
[4] D.C. Carey, et.al., SLAC-246 (1982).
[5] W.R. Nelson, H. Hirayama, D.W.O. Rogers, The EGS4 Code System, SLAC-265 (1985).
[6] Ch. Geyer, Untergrundsoptimierung der Wechselwirkungszone einer Asymmetrischen B-Mesonenfabrik, DESY M-92-02 (1992).
[7] D.C. Carey, The Optics of Charged Particle Beams, Harwood Academic Publishers (1987).
[8] B. Rossi, High-Energy Particles, Prentice-Hall (1952).
[9] E. Storm and H.I. Israel, Nucl.Data Tables A7, 565 (1970), and references therein.
[10] The detectors were manufactured by Senter for Industriforskning (Oslo/Norway).
[11] J. Stanton, A Low Power Low Noise Amplifier for a 128 Channel Read-Out Integrated Circuit, RAL-89-009 (1989).